

# Adsorption, Kinetic and Thermodynamic Studies for Mercury Extraction from Water Samples Using Mesoporous Silica

Salah Ali Mahgoub Idris

Chemistry Department, Faculty of Science, University of Tobruk, Tobruk, Libya

**Email address:**

salah.idris@ymail.com

**To cite this article:**

Salah Ali Mahgoub Idris. Adsorption, Kinetic and Thermodynamic Studies for Mercury Extraction from Water Samples Using Mesoporous Silica. *Modern Chemistry*. Vol. 7, No. 3, 2019, pp. 58-64. doi: 10.11648/j.mc.20190703.13

**Received:** August 15, 2019; **Accepted:** September 9, 2019; **Published:** September 29, 2019

---

**Abstract:** Mercury is recognized internationally as an important pollutant since mercury and its compounds are persistent, bioaccumulative and toxic, and pose human and ecosystem risks. A critical aspect of mercury cycling is its bioaccumulation, mainly as methylmercury, along the contaminated water with mercury resulting in high risk of human. Adsorption of mercury from water samples on mesoporous silica, mercaptopropyl functionalised-SBA-15 (MP-SBA-15) and diethylenetriamine functionalised-SBA-15 (DETA-SBA-15) has been studied. SBA-15 was prepared by using Pluronic P<sub>123</sub>, PEO<sub>20</sub>PPO<sub>70</sub>PEO<sub>20</sub> and tetraethylorthosilicate. Surface modification of SBA-15 was carried out by MP-TMS or DETA-TMS to produce MP-SBA-15 or DETA-SBA-15, respectively. SBA-15 and functionalised SBA-15 materials were characterised for BET surface area, pore size and pore volume. The adsorption kinetics and adsorption isotherms of functionalised SBA-15 for mercury were investigated. Results revealed that the adsorption kinetics were fitted by a pseudo-second-order reaction model and the adsorption thermodynamic parameters  $\Delta H^\circ$ ,  $\Delta S^\circ$  and  $\Delta E^\circ$  were 42.08 kJ/mol, 210.3 J/mol.K and 7.20 kJ/mol, respectively for DETA-SBA-15; 101.85 kJ/mol, 397.7 J/mol.K and 23.28 kJ/mol, respectively for MP-SBA-15. Langmuir and Freundlich isotherm models were also applied to analyse the experimental data and to predict the relevant isotherm parameters. The best interpretation for the experimental data was given by the Langmuir isotherm equation. The results indicate that the structure of the materials affects the adsorption behavior. These materials show a potential for the application as effective and selective adsorbents for Hg(II) removal from water.

**Keywords:** Mercury Sorption, Mesoporous Silica, Sorption Kinetics, Sorption Thermodynamic, Equilibrium Isotherms

---

## 1. Introduction

Mercury and its compounds act as dangerous and insidious poisons, not only through the gastrointestinal tract but also through the skin and lungs [1, 2]. The soluble compounds of mercury are particularly toxic because their absorption is very fast [3, 4]. Mercury is included in the list of priority pollutants by all environmental agencies worldwide. For example, in the United States of America, the maximum accepted concentration in drinking water is 2 µg/L [5]. On the other hand, in Japan the established values are much more restrictive with corresponding limits 0.5 µg/L [6]. The World Health Organisation (WHO) recommends a maximum uptake of 0.3 mg per week and 1 µg/L as the maximum acceptable concentration of mercury in drinking water [7].

According to those standards, the concentrations of mercury in drinking water have to be very low and in most cases the level of mercury in water and especially ground water higher than accepted concentrations [8]. To reduce the concentration from water, some separation processes have been used including; ion exchange [9], solvent extraction [10], adsorption [11], precipitation [12] and membrane separation [13]. In recent years the adsorption of mercury onto mesoporous silica to treat the drinking water from high concentration of mercury, has proved to be a valuable separation/preconcentration technique [14]. This approach provides very high concentration factors compared to conventional methods. In addition, active sites are well dispersed on its surface, and these sites are easily accessible [15]. The use of chelating agents is a promising route for

mesoporous silica surface activation, with the aim of raising its efficiency and selectivity for adsorption and pre-concentration of mercury from aqueous solutions [14].

This paper presents an assessment of mercaptopropyl functionalised-SBA-15 (MP-SBA-15) and diethylenetriamine functionalised-SBA-15 (DETA-SBA-15) for mercury extraction from water samples and study Adsorption, kinetic and thermodynamic for the mercury adsorption which can make these process more clearly, understandable and using these techniques describe the favourability and behaviour of mercury towards soft and hard ligands can be useful for optimisation analytical techniques to determine concentrations of mercury in water or for cleaning up water from high concentrations of mercury.

## 2. Experimental

### 2.1. Materials and Reagent

Pluronic P123, PEO<sub>20</sub>PPO<sub>70</sub>PEO<sub>20</sub> was supplied from BASF Corporation, tetraethoxysilane (TEOS) 98%, N-(3-trimethoxysilylpropyl) diethylenetriamine (DETA-TMS), 3-mercaptopropyltrimethoxy-silane (MP-TMS), 99%, toluene (+ 99%) and 1000 µg mL<sup>-1</sup> of Hg (II) standard solution were purchased from Sigma Aldrich. Nitric acid (HNO<sub>3</sub>, 65 wt.%), and hydrochloric acid (36%) were purchased from Fisher Scientific. Glassware was soaked in 5% HNO<sub>3</sub> overnight and

cleaned with deionised water before use. All products were used as supplied and deionised water was used throughout this work.

### 2.2. Mesoporous Silica Preparations and Functionalisation

SBA-15 was prepared using method reported in ref [16]. A surfactant tri-block copolymer solution of 4 g Pluronic P123, PEO<sub>20</sub>PPO<sub>70</sub>PEO<sub>20</sub> was dissolved in 120 cm<sup>3</sup> of 2 M hydrochloric acid and 60 cm<sup>3</sup> of distilled water in a sealed glass bottle at room temperature, and the mixture was magnetically stirred at 330 rpm. The surfactant solution was then heated to 40°C and 11.3 g of tetraethylorthosilicate (TEOS) was added and left for 24 h at 40°C. The mixture was then placed in an oven for 5 days at 60°C. The material was filtered and washed with water and dried overnight at 60°C before calcination at 550°C for 24 h.

Surface modification of SBA-15 was carried out by condensation using the organosilane of choice with SBA-15 (Figure 1). Briefly, approximately 5 g of SBA-15 was pre-treated at 140°C for 2 h before being immersed in 50 cm<sup>3</sup> of toluene and 10 cm<sup>3</sup> of MP-TMS, or DETA-TMS, in a 250 cm<sup>3</sup> flask. The mixture was refluxed for 4 h and the solid produced was filtered, washed with 100 cm<sup>3</sup> ethanol, and oven-dried at 80°C for 2 h to produce an MP-SBA-15, or DETA-SBA-15 sorbent, respectively.

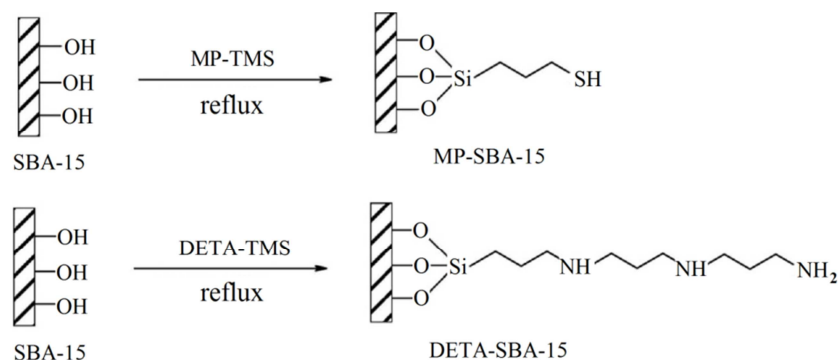


Figure 1. Modification of SBA-15 using mercaptopropyltrimethoxy-silane and N-(3-trimethoxysilylpropyl) diethylenetriamine.

### 2.3. Characterisation and Analysis

The surface area of the SBA-15 and functionalised-SBA-15 were measured using nitrogen physisorption isotherms on a Micromeritics Gemini 2375 volumetric analyser. Each sample was degassed prior to analysis for 6 h at 200°C. The Brumauer–Emmett–Teller (BET) surface areas were calculated using experimental points at a relative pressure (P/P<sub>0</sub>) of 0.05–0.25. The total pore volume was calculated from the N<sub>2</sub> amount adsorbed at the P/P<sub>0</sub> of 0.99 for each sample and the average pore size distribution of the materials was calculated using the Barrett–Joyner–Halanda (BJH) model from a 30-point BET surface area plot. All samples exhibited a Type IV adsorption isotherm typical of mesoporous solids. Desorption isotherms were used to calculate the pore diameters. Infrared spectra of all samples were obtained in KBr pellets in the 4000–400 cm<sup>-1</sup> region

with a resolution of 4 cm<sup>-1</sup>, by accumulating 64 scans using an ATI Mattson FTIR spectrophotometer. Elemental analysis (EA) was carried out using an Exeter Analytical CE440 elemental function. Total concentrations of mercury in water samples were determined by inductivity coupled plasma atomic emission spectrometry (ICP-AES) using a Perkin Elmer Optima 5300DV instrument (Perkin Elmer, UK) at an RF power of 1300 W and with plasma, auxiliary and nebuliser argon gas flows of 15, 0.2 and 0.75 L min<sup>-1</sup> respectively, and a pump flow rate of 1.5 mL min<sup>-1</sup> and analytical precision (RSD) was typically 1-5% for individual aliquots (n=3).

### 2.4. Adsorption Isotherms

The Langmuir [17] or Freundlich [18] models were applied to measured data to study adsorption isotherms.

Solutions containing initial concentrations of Hg at 10, 50, 100 or 200  $\mu\text{g cm}^{-3}$  were prepared. To each solution 0.05 g of sorbent was added and the solution was stirred at 250 rpm for 120 min at room temperature, solutions were adjusted to provide a pH of 7. The amounts of Hg extracted at equilibrium,  $q_e$  (mg/g) were calculated according to Eq. (1):

$$q_e = \frac{C_0 - C_e}{W} V \quad (1)$$

where  $C_0$  and  $C_e$  (mg/g) were the liquid phase initial and equilibrium concentrations of the Hg respectively.  $V$  was the volume of the solution ( $\text{cm}^3$ ), and  $W$  was the mass of sorbent (g) used [19]. The sorption equilibrium data were analysed according to Langmuir Eq. (2) and Freundlich Eq. (3) isotherm models [20].

$$\frac{C_e}{q_e} = \left( \frac{1}{q_m b} \right) + \left( \frac{1}{q_m} \right) C_e \quad (2)$$

$$\ln q_e = \ln K_f + \left( \frac{1}{n} \right) \ln C_e \quad (3)$$

where  $q_e$  and  $C_e$  were the equilibrium concentrations of the Hg ions in the adsorbed and liquid phases in mg/g and mg/L, respectively.  $q_m$  (mg/g) and  $b$  (L/mg) were the Langmuir constants. Whereas the  $q_m$  is the maximum monolayer capacity and  $b$  was the adsorption affinity onto the adsorption.  $K_f$  (mg/g) and  $n$  (L/mg) were the Freundlich constants which are related to the sorption capacity and intensity, respectively. The Langmuir and Freundlich constants were calculated from the slope and intercept of the linear plot obtained from eq. 2 and 3 respectively.

For predicting the favorability of an adsorption system, the Langmuir equation can also be expressed in terms of a dimensionless separation factor ( $R_L$ ) by using the Langmuir constant  $b$  and the initial concentrations of the mercury (Eq. 4).

$$R_L = \frac{1}{1 + C_0 b} \quad (4)$$

When,  $R_L > 1$ ,  $R_L = 1$ ,  $0 < R_L < 1$  and  $R_L = 0$ , indicates unfavourable, linear, favourable and irreversible, adsorption isotherms, respectively [21, 22].

## 2.5. Adsorption Kinetics Study

Kinetic studies to determine the rate of Hg removal from water samples were conducted for MP-SBA-15 and DETA-SBA-15. Solutions were prepared with the same initial Hg concentration of 10  $\mu\text{g cm}^{-3}$  and stirred with 0.05 g of each sorbent at 250 rpm. 25  $\text{cm}^3$  aliquots of each solution were stirred at 25°C for 1, 5, 10, 20, 30 or 40 min. After each time period, solutions were filtered and analysed by ICP-AES to determine the concentration of Hg in the final solution. The kinetics of Hg adsorption onto the surface of the silica nanoparticles were analysed using pseudo first-order [23], pseudo second-order [24] and intraparticle diffusion [25, 26] kinetic models. The conformity between experimental data and the model predicted values was expressed by the correlation coefficients ( $R^2$ ). A relatively high  $R^2$  value (close or equal to 1) was used to indicate best fit to the kinetic

model.

*The pseudo first-order equation:*

The pseudo first-order equation is generally presented as follows:

$$\log(q_e - q_t) = \log(q_e) - \frac{k_1}{2.303} t \quad (5)$$

where  $q_e$  and  $q_t$  are the adsorption capacity at equilibrium and at time  $t$ , respectively ( $\text{mg g}^{-1}$ ),  $k_1$  is the rate coefficient of pseudo first-order adsorption ( $\text{L min}^{-1}$ ). The plot of  $\log(q_e - q_t)$  vs.  $t$  should give a linear relationship from which  $k_1$  and  $q_e$  can be determined from the slope and intercept of the plot, respectively.

*The pseudo second-order equation:*

The pseudo second-order adsorption kinetic rate equation is expressed as:

$$\left( \frac{t}{q_t} \right) = \frac{1}{k_2 q_e^2} + \frac{1}{q_e} t \quad (6)$$

where  $k_2$  is the rate coefficient of pseudo second-order adsorption ( $\text{g mg}^{-1} \text{min}^{-1}$ ). The plot of  $\left( \frac{t}{q_t} \right)$  and  $t$ , should give a linear relationship from which  $q_e$  and  $k_2$  can be determined from the slope and intercept of the plot, respectively.

*The intraparticle diffusion model:*

To study the mechanism of the particle diffusion the Morris–Weber equation was applied:

$$q_t = k_{id} \sqrt{t} \quad (7)$$

where  $q_t$  is the amount of metal ion sorbed ( $\text{mg L}^{-1}$ ) at time  $t$  and  $k_{id}$  is the intraparticle diffusion rate coefficient ( $\text{mg L}^{-1} \text{min}^{-1/2}$ ).

## 2.6. Thermodynamic Study

Thermodynamic studies for Hg removal from water samples were conducted for MP-SBA-15 and DETA-SBA-15. Solutions were prepared with the same initial Hg concentration of 50  $\mu\text{g cm}^{-3}$  and stirred with 0.05 g of each sorbent at 250 rpm. 25  $\text{cm}^3$  aliquots of each solution were stirred at 25, 35, 45 and 55°C for 1, 5, 10, 20, 30 or 40 min. After each time period, solutions were filtered and analysed by ICP-AES to determine the concentration of Hg in the final solution.

The free energy ( $\Delta G^\theta$ ) of the adsorption reaction is given by the following equation:

$$\Delta G^\theta = -RT \ln K_c \quad (8)$$

where  $K_c$  is the adsorption equilibrium constant,  $R$  is the gas constant and  $T$  is the absolute temperature (K). The adsorption equilibrium constant ( $K_c$ ) can be calculated from:

$$K_c = \frac{F_e}{1 - F_e} \quad (9)$$

where  $F_e$  is the fraction attainment of mercury ion adsorbed at equilibrium time, and is obtained by the expression

$$F_e = \frac{C_0 - C_e}{C_0} \quad (10)$$

where  $C_0$  and  $C_e$  are the initial and equilibrium concentrations of mercury ion in solution (mg/L). The value of the adsorption equilibrium constant ( $K_c$ ) for the adsorption of mercury ion on the adsorbent were calculated at different temperature and at equilibrium time using Eqs. (9) and (10). The Gibbs free energy can be represented as follows:

$$\Delta G^0 = \Delta H^0 - T\Delta S^0 \quad (11)$$

The values of enthalpy change ( $\Delta H^0$ ) and entropy change ( $\Delta S^0$ ) calculated from the intercept and slope of the plot of  $\Delta G^0$  versus  $T$  [27].

The activation energy for mercury adsorption was calculated by the Arrhenius equation

$$k_2 = Ae^{(-\frac{\Delta E}{RT})} \quad (12)$$

where  $\Delta E$  is the activation energy (kJ/mol),  $A$  is the frequency factor,  $T$  is the absolute temperature (K), and  $R$  is the gas constant. From the plot of  $\ln(k_2)$  vs.  $1/T$ , the activation energy  $\Delta E$  for the adsorption of mercury can be calculated.

### 3. Results and Discussion

#### 3.1. Materials Characterisation

The SBA-15 and Functionalised-SBA-15 materials were characterised using BET to examine their pore size and surface area. The physicochemical properties of each material are summarised in Table 1.

Table 1. Physicochemical properties of mesoporous materials used.

Sample Name	BET Surface Area ( $\text{m}^2 \text{g}^{-1}$ ) <sup>a</sup>	Pore Size (nm) <sup>b</sup>	Pore Volume ( $\text{cm}^3 \text{g}^{-1}$ ) <sup>c</sup>
SBA-15	950.6	7.25	1.14
MP-SBA-15	578.1	6.84	0.841
DETA-SBA-15	328.7	6.14	0.644

<sup>a</sup> Calculated by the BJH model from sorption data in a relative pressure range from 0.05–0.25.

<sup>b</sup> Calculated by the BJH model from the adsorption branches of isotherms.

<sup>c</sup> Calculated from  $\text{N}_2$  amount adsorbed at a relative pressure  $P/P_0$  of 0.99.

Table 2. Elemental analysis data recorded for the SBA-15.

Silica	% C	% H	% N	% S	$L_o$ (mmol/g) <sup>a</sup>
SBA-15	Trace/Nil	0.65	Trace/Nil	Trace/Nil	.....
MP-SBA-15	12.68	2.33	Trace/Nil	10.21	3.19
DETA-SBA-15	18.43	4.92	11.07	0.00	7.91

<sup>a</sup> Functionalisation degree ( $L_o$  = millimoles of ligand per gram of functionalised silica)

The FTIR spectra of all samples (Figure 3) contain similar features expected of a silica containing material associated with the inorganic backbone such as, a large broad band between 3500 and 3200  $\text{cm}^{-1}$  which is assigned to the O–H stretching mode of silanol groups and also to some adsorbed water, and several absorption bands at around 1030–1240  $\text{cm}^{-1}$  which can be assigned to the Si–O–Si stretching and the water bending mode band around 1650  $\text{cm}^{-1}$ .

In addition to those peaks the spectrum of the MP-SBA-15

The  $\text{N}_2$  sorption isotherms (Figure 2) were type IV for all samples confirming their mesoporous natures, however different volumes of nitrogen gas adsorbed on the mesoporous silica surfaces were noted at higher relative pressures for SBA-15 compared with MP-SBA-15, and DETA-SBA-15 suggesting large of the surface are occupied by functional groups.

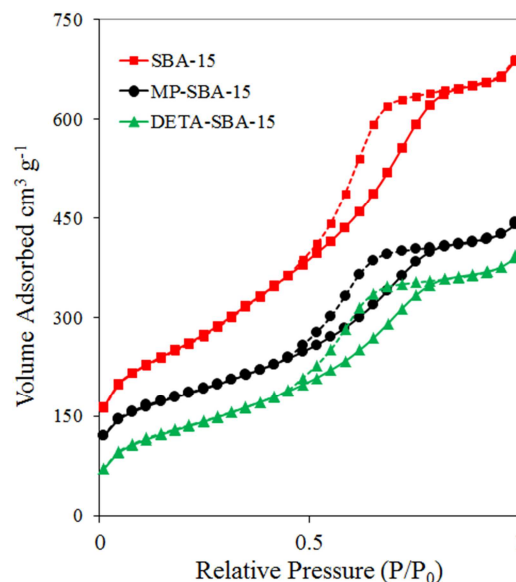


Figure 2. Nitrogen adsorption isotherms for mesoporous silica sorbents.

Elemental analysis was used to estimate the amount of molecules ( $L_o$ ) attached to functionalised samples from the percentage of nitrogen or sulphur, in the functionalised mesoporous silica [28], using equation (13):

$$L_o = \frac{\% N}{\text{nitrogen or sulphur atomic weight}} \times 10 \quad (13)$$

The calculated  $L_o$  (Table 2) values for MP-SBA-15 and DETA-SBA-15 were high indicating the successfully functionalisation for mercaptopropyl and diethylenetriamine functional groups.

sample contained extra band at 2850 and 2930  $\text{cm}^{-1}$  which were assigned to the C–H stretching of  $\text{sp}^3$  carbon, and a weak band at 2557  $\text{cm}^{-1}$  was assigned to a SH stretching mode, supporting the theory that MP is present on the surface of the silica. DETA-SBA-15 sample contained extra bands which were assigned to N–H stretch at 1470  $\text{cm}^{-1}$  and in the range 1340–1400  $\text{cm}^{-1}$ ; which can be assigned as a secondary C–N stretch which was an indication for functionalization of the silica surface. [29].

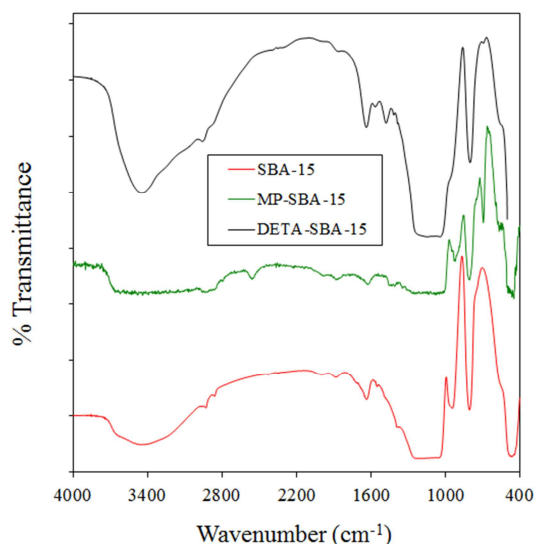


Figure 3. FTIR spectra of SBA-15, MP-SBA-15 and DETA-SBA-15.

### 3.2. Adsorption Isotherms

The adsorption isotherms were studied to find the relationship between equilibrium adsorption capacity and equilibrium concentration at a certain temperature.

Langmuir and Freundlich isotherms are the most commonly used isotherms for different adsorbent/adsorbate systems to explain solid-liquid adsorption systems and to predict their equilibrium parameters [30-32]. The relevant parameters for these isotherms are presented in table 3. As seen from table 3, the  $R^2$  values obtained from the Langmuir model are much closer to one than are those from the Freundlich model, suggesting that the Langmuir model is better than the Freundlich isotherm. Thus the adsorption can be described by the Langmuir isotherm and the metal ion adsorption occurs on a homogeneous surface by monolayer sorption without interaction between the adsorbed ion [33].

Table 3. Isotherm parameters for mercury sorption on functionalised mesoporous silica.

Adsorbents	Langmuir				Freundlich		
	$q_m$ (mg/g)	$b$ (L/mg)	$R_L$	$R^2$	$K_f$ (mg/g)	$n$ (L/mg)	$R^2$
DETA-SBA-15	38.6	0.74	0.93	0.9982	24.9	6.70	0.6728
MP-SBA-15	108.7	1.88	0.84	0.8900	58.3	1.94	0.8806

### 3.3. Adsorption Kinetics

The experimental kinetic data were fitted using a pseudo-first order kinetic model and pseudo-second-order kinetic model. The results are shown in table 4. It can be seen that the obtained  $R^2$  values of the pseudo-second-order model ( $> 0.994$ ) were better than those of the pseudo-first order model (0.903-0.992) for both adsorbents, suggesting that the adsorption process is second-order. Moreover, the calculated

$q_e$  values were much closer to the experimental values in the pseudo-second-order kinetic model than the pseudo-first order kinetic model indicating that the adsorption process is second-order. As seen in table 4, when the initial ion concentration increases from 10 to 200  $\mu\text{g/ml}$ , the pseudo-second-order constants ( $k_2$ ) decrease from 0.811 to 0.010, 0.461 to 0.010 for DETA-SBA-15 and MP-SBA-15, respectively. This indicates that the available active sites on the adsorbents are saturated rapidly by mercury ion.

Table 4. Kinetic parameters for the adsorption of mercury on the adsorbent.

Adsorbents	$C_0$ $\mu\text{g/mL}$	$q_e$ (exp) (mg/g)	The pseudo first-order			The pseudo second-order		
			$k_1$ ( $\text{min}^{-1}$ )	$q_e$ (cal) (mg/g)	$R^2$	$k_2$ ( $\text{min}^{-1}$ )	$q_e$ (cal) (mg/g)	$R^2$
DETA-SBA-15	10	5.00	0.204	1.25	0.9606	0.811	5.03	0.9999
DETA-SBA-15	50	25.00	0.204	12.37	0.9923	0.062	25.44	0.9995
DETA-SBA-15	100	33.50	0.076	18.67	0.9662	0.016	33.99	0.9942
DETA-SBA-15	200	38.50	0.075	4.47	0.9038	0.106	38.47	0.9998
MP-SBA-15	10	4.99	0.219	1.99	0.9547	0.461	5.05	0.9995
MP-SBA-15	50	24.97	0.231	19.53	0.9417	0.045	25.56	0.9989
MP-SBA-15	100	49.50	0.138	35.36	0.9933	0.013	51.09	0.9971
MP-SBA-15	200	98.60	0.158	58.16	0.9842	0.010	101.14	0.9985

Adsorption capacity is more for MP-SBA-15 compared with DETA-SBA-15 due to large surface area, favourability of mercury to bonded to soft ligand as mercury is soft metal and also may be due to the adsorption of mercury inside pores which may not the case with DETA-SBA as the sterical hindered occurs because the length of the chain in the functional groups.

Figure 4 shows the intraparticle diffusion model for mercury adsorption onto MP-SBA-15 and DETA-SBA-15.

The amount adsorbed of mercury ions from aqueous solutions on the adsorbent at different concentrations as a function of reaction time. The figure shows a higher initial rate of removal within the first 10 minutes followed by a slower subsequent removal rate till reaching equilibrium. With increasing the initial concentration the slower adsorption process was observed in both sorbents but both are reached in 20 minutes in all cases.



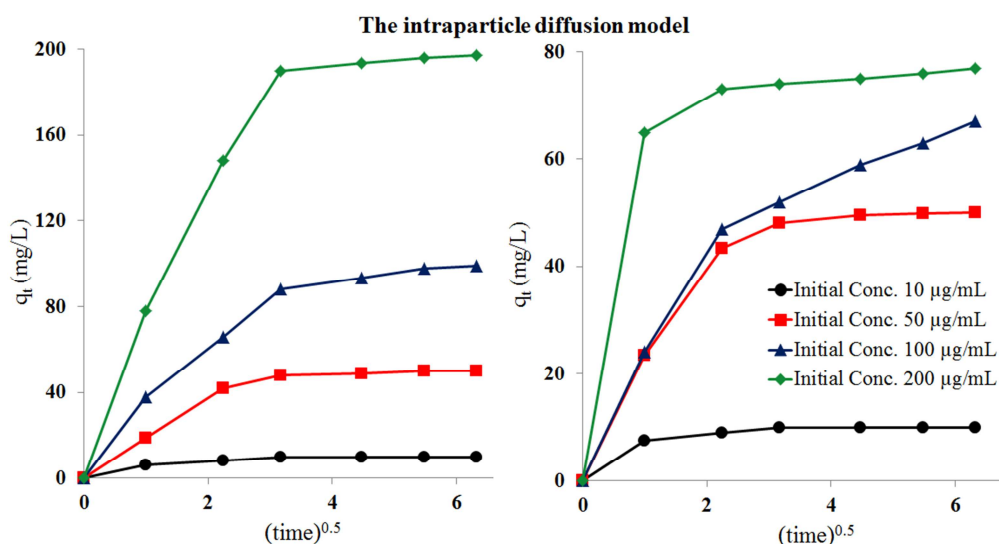


Figure 4. The intraparticle diffusion model for mercury adsorption onto MP-SBA-15 and DETA-SBA-15.

### 3.4. Adsorption Thermodynamics

The thermodynamic parameters of the adsorption process, such as free energy ( $\Delta G^0$ ) of the adsorption, enthalpy change ( $\Delta H^0$ ) and entropy change ( $\Delta S^0$ ) and activation energy ( $\Delta E$ ) were determined and are listed in table 5. The variation of equilibrium constant ( $K_c$ ) with temperature, as summarised in table 5, showed that  $K_c$  values were increased with increase in adsorption temperature, thus implying a strengthening of adsorbate-adsorbent interactions at higher temperature.

Negative values of  $\Delta G^0$  confirm that the process is endothermic and spontaneous. The value of  $\Delta H^0$  was found to be positive confirming the endothermic nature of the adsorption process. The positive values of  $\Delta S^0$  show the increased randomness at the solid/solution interface with some structural changes in the adsorbate and adsorbent. The activation energy values for the adsorption of mercury were found to be 7.20 kJ/mol and 23.28 kJ/mol for DETA-SBA-15 and MP-SBA-15, respectively.

Table 5. Thermodynamic parameters for the adsorption of mercury on the adsorbent.

Adsorbents	Reaction Temp. (K)	$K_c$	$\Delta G^0$ (kJ/mol)	$\Delta H^0$ (kJ/mol)	$\Delta S^0$ (J/mol.K)	$\Delta E^0$ (kJ/mol)
DETA-SBA-15	298	4999	-21.10	42.08	210.3	7.20
DETA-SBA-15	308	6249	-22.38			
DETA-SBA-15	318	8332	-23.87			
DETA-SBA-15	328	24999	-27.62			
MP-SBA-15	298	832	-16.66	101.85	397.7	23.28
MP-SBA-15	308	4545	-21.57			
MP-SBA-15	318	5556	-22.80			
MP-SBA-15	328	49999	-29.51			

## 4. Conclusions

In this study, MP-SBA-15 and DETA-SBA-15 were prepared and the adsorption of mercury ions by these adsorbents was investigated. The equilibrium data well fitted the Langmuir sorption isotherms ( $R^2$  values are closer to one), and the maximum adsorption capacity of mercury reached 38.6 mg/g and 108.7 mg/g for DETA-SBA-15 and MP-SBA-15, respectively. The adsorption process is fitted by pseudo-second-order kinetic model and the adsorption thermodynamic parameters revealed that the uptake reactions of mercury to adsorbents are spontaneous and endothermic. These results show a high potential for application in mercury clean-up of contaminated waters, in particular, it is due to the high mercury uptake especially with MP-SBA-15. It is important to note that the adsorption capacities of the adsorbents presented

in this paper vary, depending on the characteristics of the individual adsorbent, the extent of chemical modifications.

## References

- [1] L. A. Belyakova, O. M. Shvets, D. Y. e. Lyashenko, *Inorganica Chimica Acta*, 362 (2009) 2222-2230.
- [2] I. M. M. Kenawy, Y. G. Abou El-Reash, M. M. Hassanien, N. R. Alnagar, W. I. Mortada, *Microporous and Mesoporous Materials*, 258 (2018) 217-227.
- [3] J. Lu, X. Wu, Y. Li, W. Cui, Y. Liang, *Surfaces and Interfaces*, 12 (2018) 108-115.
- [4] Y. Fu, J. Jiang, Z. Chen, S. Ying, J. Wang, J. Hu, *Journal of Molecular Liquids*, 286 (2019) 110746.
- [5] USEPA, National Primary DrinkingWater Standards, Report EPA/625/R-97/004, in, Washington DC, 2001.

- [6] J. Takahashi, K. Watanuki, S. Kubota, O. Wada, Y. Arikawa, S. Naito, S. Monma, T. Hirato, An Encyclopedia of Water, in, Maruzen Publishing Co., Tokyo, 2001.
- [7] C. Foster, J. Wase, Biosorbents for Metal Ions, Taylor & Francis, New York, 1997.
- [8] Y. Fu, Y. Sun, Z. Chen, S. Ying, J. Wang, J. Hu, Science of The Total Environment, 691 (2019) 664-674.
- [9] A. A. Khan, Inamuddin, Sensors and Actuators B: Chemical, 120 (2006) 10-18.
- [10] Z. Li, Q. Wei, R. Yuan, X. Zhou, H. Liu, H. Shan, Q. Song, Talanta, 71 (2007) 68-72.
- [11] X. Lu, J. Jiang, K. Sun, J. Wang, Y. Zhang, Marine Pollution Bulletin, 78 (2014) 69-76.
- [12] J. Zhou, X. Feng, H. Liu, H. Zhang, X. Fu, Z. Bao, X. Wang, Y. Zhang, Atmospheric Environment, 81 (2013) 364-372.
- [13] K. Chakrabarty, P. Saha, A. K. Ghoshal, Journal of Membrane Science, 350 (2010) 395-401.
- [14] S. A. Idris, S. R. Harvey, L. T. Gibson, Journal of Hazardous Materials, 193 (2011) 171-176.
- [15] M. Shafiabadi, A. Dashti, H.-A. Tayebi, Synthetic Metals, 212 (2016) 154-160.
- [16] S. A. Idris, C. Robertson, M. A. Morris, L. T. Gibson, Analytical Methods, 2 (2010) 1803-1809.
- [17] I. Langmuir, J. Am. Chem. Soc., 40 (1918) 1361-1403.
- [18] J.-u.-R. Memon, S. Q. Memon, M. I. Bhanger, M. Y. Khuhawar, J. Hazard. Mater., 163 (2009) 511-516.
- [19] G. Purna Chandra Rao, S. Satyaveni, A. Ramesh, K. Sessaiah, K. S. N. Murthy, N. V. Choudary, Journal of Environmental Management, 81 (2006) 265-272.
- [20] G. Zolfaghari, A. Esmaili-Sari, M. Anbia, H. Younesi, S. Amirmahmoodi, A. Ghafari-Nazari, Journal of Hazardous Materials, 192 (2011) 1046-1055.
- [21] T. Y. Guo, Y. Q. Xia, G. J. Hao, M. D. Song, B. H. Zhang, Biomaterials, 25 (2004) 5905-5912.
- [22] J. Pan, X. Zou, X. Wang, W. Guan, Y. Yan, J. Han, Chem. Eng. J. (Lausanne), 162 (2010) 910-918.
- [23] S. Lagergren, Handlingar, 24 (1898) 1-39.
- [24] Y. Ho, G. McKay, D. Wase, C. Foster, Adsorption Science and Technology 18 (2000) 639-650.
- [25] S. Srivastava, R. Tygir, N. Pant, Water Res., 23 (1989) 1161-1165.
- [26] W. Weber, J. Morris, Am. Soc. Civ. Eng., 89 (1963) 31-60.
- [27] T. Wajima, K. Sugawara, Fuel Processing Technology, 92 (2011) 1322-1327.
- [28] D. Pérez-Quintanilla, I. d. Hierro, M. Fajardo, I. Sierra, J. Hazard. Mater., 134 (2006) 245-256.
- [29] J. Coates, Interpretation of Infrared Spectra, A Practical Approach, in: Encyclopedia of Analytical Chemistry, John Wiley & Sons, Ltd, 2006.
- [30] Y.-S. Ho, W.-T. Chiu, C.-S. Hsu, C.-T. Huang, Hydrometallurgy, 73 (2004) 55-61.
- [31] Y.-S. Ho, Water Research, 37 (2003) 2323-2330.
- [32] S. Hong, C. Wen, J. He, F. Gan, Y.-S. Ho, Journal of Hazardous Materials, 167 (2009) 630-633.
- [33] Y. Sağ, Y. Aktay, Process Biochemistry, 36 (2001) 1187-1197.